Anti–PD-1/anti–CTLA-4 efficacy in melanoma brain metastases depends on extracranial disease and augmentation of CD8+ T cell trafficking

David Taggart[a,b], Tereza Andreou[a], Karen J. Scott[a], Jennifer Williams[a], Nora Rippaus[a], Rebecca J. Brownlie[a], Elizabeth J. Ilett[a], Robert J. Salmond[a], Alan Melcher[a,c], and Mihaela Lorger[a,1]

[a]Leeds Institute of Cancer and Pathology, University of Leeds, Leeds LS9 7TF, United Kingdom; [b]MRC Centre for Inflammation Research, University of Edinburgh, Edinburgh EH8 9YL, United Kingdom; and [c]The Institute of Cancer Research, The Royal Marsden NHS Foundation Trust, London SW3 6JJ, United Kingdom

Inhibition of immune checkpoints programmed death 1 (PD-1) and cytotoxic T lymphocyte-associated protein 4 (CTLA-4) on T cells results in durable antitumor activity in melanoma patients. Despite high frequency of melanoma brain metastases (BrM) and associated poor prognosis, the activity and mechanisms of immune checkpoint inhibitors (ICI) in metastatic tumors that develop within the "immune specialized" brain microenvironment, remain elusive. We established a melanoma tumor transplantation model with intracranial plus extracranial (subcutaneous) tumor, mimicking the clinically observed coexistence of metastases inside and outside the brain. Strikingly, intracranial ICI efficacy was observed only when extracranial tumor was present. Extracranial tumor was also required for ICI-induced increase in CD8+ T cells, macrophages, and microglia in brain tumors, and for up-regulation of immune-regulatory genes. Combined PD-1/CTLA-4 blockade had a superior intracranial efficacy over the two monotherapies. Cell depletion studies revealed that NK cells and CD8+ T cells were required for intracranial anti–PD-1/anti–CTLA-4 efficacy. Rather than enhancing CD8+ T cell activation and expansion within intracranial tumors, PD-1/CTLA-4 blockade dramatically (~14-fold) increased the trafficking of CD8+ T cells to the brain. This was mainly through the peripheral expansion of homing-competent effector CD8+ T cells and potentially further enhanced through up-regulation of T cell entry receptors intercellular adhesion molecule 1 and vascular adhesion molecule 1 on tumor vasculature. Our study indicates that extracranial activation/release of CD8+ T cells from PD-1/CTLA-4 inhibition and potentiation of their recruitment to the brain are paramount to the intracranial anti–PD-1/anti–CTLA-4 activity, suggesting augmentation of these processes as an immune therapy-enhancing strategy in metastatic brain cancer.

anti–PD-1 | anti–CTLA-4 | melanoma | brain metastases | T cell trafficking

Brain metastases (BrM) are an unmet clinical need with very limited treatment options and poor prognosis. Metastatic melanoma has the highest risk of spreading to the central nervous system (CNS) among common cancers; up to a quarter of patients have BrM at metastatic diagnosis, and the incidence at autopsy is up to ~75% (1–3). Until recently, treatment options for melanoma BrM have been restricted to radiotherapy, surgery, and targeted therapies, with the median overall survival below 1 y (4, 5). In recent years, cancer treatment has been revolutionized by immunotherapy targeting programmed death 1 (PD-1) and cytotoxic T lymphocyte-associated protein 4 (CTLA-4) immune-inhibitory receptors (immune checkpoints) expressed mainly on T cells. Function-blocking antibodies against CTLA-4 (ipilimumab) and PD-1 (nivolumab, pembrolizumab) enhance antitumor T cell responses and result in durable antitumor activity across most cancers (6, 7). In melanoma, the anti–PD-1/anti–CTLA-4 combination therapy showed a superior efficacy compared with the two monotherapies (8), and has been approved in various countries (9). Despite numerous studies on anti–PD-1 and anti–CTLA-4 in melanoma, very limited data are

available for BrM, mainly due to frequent exclusion of patients with BrM from clinical trials (4, 10). A handful of retrospective and prospective clinical studies indicated activity of ipilimumab in melanoma BrM with 16–25% intracranial response rate, but also suggested that only a subgroup of patients is likely to benefit (4, 5, 11). Pembrolizumab and nivolumab also showed efficacy in melanoma BrM with an ~21% response rate in the brain (12–15). A very recent interim analyses from two clinical trials in drug treatment-naïve patients with melanoma BrM [ABC trial (15) and CheckMate 204 trial (16)] reported a 50% and 55% intracranial response rate following combined anti–PD-1 plus anti–CTLA-4 therapy.

In addition to limited clinical data, there is a complete lack of preclinical data on anti–PD-1 and anti–CTLA-4 therapy in melanoma BrM. Preclinical studies in BrM are hampered by the lack of melanoma models that can recapitulate clinically observed metastatic patterns and coexistence of metastases in different organs. Spontaneous metastasis to the brain in preclinical models is a rare event and macroscopic BrM are usually not observed (17). Only two immunocompetent preclinical melanoma models of spontaneous BrM have been reported (18, 19), but analysis of BrM-specific survival in therapeutic studies

---

Significance

Brain metastases are an unmet clinical need with high frequency in melanoma patients. With immune checkpoint inhibitors targeting programmed death 1 (PD-1) and cytotoxic T lymphocyte-associated protein 4 (CTLA-4) becoming a frontline therapy in melanoma, it is critical to understand how this therapy works in the "immune-specialized" brain microenvironment. Our study shows that in the absence of extracranial tumor, melanoma tumors growing in the brain escape anti–PD-1/anti–CTLA-4 therapy. A synergy between immune checkpoint inhibition and extracranial tumor is required to put a break on brain metastases by enhancing CD8+ T cell recruitment to the brain via peripheral expansion of effector cells and upregulation of T cell entry receptors on tumor blood vessels. Augmentation of these processes could be explored to enhance the efficacy of immunotherapy in brain metastases.

---

remains a challenge due to a faster development of extracranial compared with intracranial metastases.

Notably, differences in regulation of adaptive T cell responses to antigens located in the CNS compared with antigens outside the CNS have been well documented (20–24). Due to this difference in adaptive immune responses, the CNS has been referred to as "immune specialized." Moreover, the phenotype of immune cells infiltrating brain metastases has been shown to be altered by inflammatory molecules up-regulated specifically in cancer cells growing in the brain parenchyma (25). Hence, with immune checkpoint inhibitors (ICI) now being frontline therapy for metastatic melanoma, the question arises as to what extent the metastatic tumors residing within the immune specialized brain microenvironment respond to ICI. Moreover, the requirements for effective anti–PD-1/anti–CTLA-4 therapy in the brain remain to be identified.

To address the above knowledge gaps and study anti–PD-1/anti–CTLA-4–dependent survival and mechanisms specifically in BrM while simulating the clinically observed coexistence of metastasis in the skin [the most common metastatic site (26)], we established a melanoma transplantation model with extracranial (subcutaneous) plus intracranial tumors, in which the overall survival depends on the intracranial tumor growth. In addition to demonstrating a superior intracranial efficacy of combined PD-1/CTLA-4 blockade over the two monotherapies, we made a striking observation that anti–PD-1/anti–CTLA-4 activity in the brain depends on the presence of extracranial tumor, highlighting the importance of mimicking clinically observed extracranial disease in the context of ICI studies. We further show that the intracranial activity of anti–PD-1/anti–CTLA-4 therapy requires the augmentation of $CD8^+$ T cell trafficking to the brain and we analyze the underlying mechanisms.

Results

The Presence of Extracranial Tumor Is Critical for Intracranial Anti–PD-1/Anti–CTLA-4 Efficacy.
The vast majority of BrM in melanoma coincide with metastases outside the brain, predominantly in the skin (26). To mimic this clinical situation, we established a tumor transplantation model of B16 melanoma with extracranial (subcutaneous) plus intracranial tumors. To identify the optimal experimental timeline allowing us to study survival specifically in dependence of intracranial tumor growth, we first determined tumor growth kinetics and survival times in mice bearing either extracranial or intracranial tumors (Fig. 1A and Fig. S1 A and B). The mean survival time for mice with intracranial tumors was 10.8 ± 1.5 d. Extracranial tumors reached the maximum allowable diameter of 15 mm on day 16.5 ± 1.4 and none of the mice showed terminal symptoms at this time point. Thus, subcutaneous implantation of cancer cells into the flank 3 d before their intracranial implantation (Fig. 1B) allowed for quantification of the intracranial tumor-dependent survival.

Following administration of four doses of either anti–CTLA-4 or anti–PD-1 antibody monotherapy (Fig. 1B), the overall survival of mice in this model was only marginally and nonsignificantly extended compared with control mice receiving IgG isotype antibody (Fig. 1C and Fig. S1C). In contrast to monotherapies, the anti–PD-1/anti–CTLA-4 combination significantly prolonged survival in our model and inhibited intracranial as well as extracranial tumor growth (Fig. 1 C–E and Fig. S1C). Thus, the outcome of anti–PD-1/anti–CTLA-4 combination therapy was superior to the two monotherapies, which is in line with the reported clinical intracranial response rate for anti–PD-1 monotherapy (21–25%) (12–15) and anti–PD-1/anti–CTLA-4 combination therapy (50–55%) (15, 16), as well as the 6-mo progression-free survival rate of 28% and 46%, respectively (15). Due to these promising data, we focused on the anti–PD-1/anti–CTLA-4 combination therapy.

To validate the relevance of extracranial disease in the context of anti–PD-1/anti–CTLA-4 therapy for BrM, we compared therapeutic efficacy between mice bearing intracranial tumors only [representing a conventional intracranial tumor transplantation model (17, 27)], and mice bearing tumors at both sites. Strikingly, in the absence of extracranial disease, the anti–PD-1/anti–CTLA-4 combination failed to extend the survival or to reduce the intracranial tumor burden (Fig. 1 F–H and Fig. S1 D and E). This observation reproduced in a B16 model overexpressing an immunogenic ovalbumin (OVA) xenoantigen (28), hence demonstrating that increasing the inherent immunogenicity of the model is not sufficient to induce antitumor responses in the brain following PD-1/CTLA-4 blockade (Fig. 1I). The requirement of extracranial disease for intracranial anti–PD-1/anti–CTLA-4 efficacy was further confirmed in the Ret melanoma model (19, 29), demonstrating that our findings are model-independent (Fig. 1J; see Fig. S1 F–H for the establishment of experimental timeline in Ret model). Taken together, our results reveal that the intracranial activity of anti–PD-/anti–CTLA-4 depends on the extracranial tumor, highlighting the importance of including the clinically relevant extracranial disease in this context.

Immune Response in the Brain Is Enhanced in the Presence of Extracranial Disease.
To evaluate the immunological response in the brain upon anti–PD-1/anti–CTLA-4 therapy and the role of extracranial disease, we analyzed the tumor-infiltrating immune cells in intracranial B16 tumors by flow cytometry (Fig. S2A). Although anti–PD-1/anti–CTLA-4 therapy resulted in a small increase in intratumoral $CD45^+$ cells in the absence of extracranial disease, a major anti–PD-1/anti–CTLA-4–induced increase in this cell population, and significant expansion of $CD3^+$ T cells, were observed only in the presence of subcutaneous tumor (Fig. 2 A–C and Fig. S2B). Similarly, anti–PD-1/anti–CTLA-4–induced increases in $CD8^+$ T cells (Fig. 2D), $CD11b^+F4/80^+CD45^{high}$ (25, 30, 31) bone marrow-derived macrophages (Fig. 2G) and $CD11b^+F4/80^+CD45^{low}$ (25, 30, 31) brain-resident microglia (Fig. 2H) were detected only in the presence of extracranial disease. In contrast, the percentages of total $CD4^+$ T cells, $FoxP3^+CD4^+$ regulatory T cells (T_{reg}) and $FoxP3^-CD4^+$ effector T cells (T_{eff}) increased upon anti–PD-1/anti–CTLA-4 treatment independent of extracranial tumor (Fig. 2D). The $CD4^+T_{eff}/T_{reg}$ ratio, the increase of which was previously associated with therapeutic efficacy in some studies (32), remained unaltered (Fig. 2E). The proportion of NK cells also remained unchanged (Fig. 2F). Importantly, similar changes in immune cell populations within intracranial tumors were observed in the Ret melanoma model (Fig. S3A).

To determine whether monotherapies are sufficient to induce infiltration of immune cells into intracranial tumors, we analyzed immune cell populations in mice bearing intracranial and extracranial B16 tumors, following anti–PD-1 or anti–CTLA-4 monotherapy. Both monotherapies failed to increase the proportion of immune cells in intracranial tumors compared with IgG-treated mice (Fig. S3B). Thus, the lack of therapeutic efficacy observed for the two monotherapies was in line with their failure to induce immune cell infiltration into intracranial tumors.

To evaluate the immunological response in the brain at the molecular level, intracranial B16 tumors were profiled using next-generation RNA sequencing (mRNAseq). Differential gene-expression analysis (adjusted $P < 0.05$) indicated that the presence of extracranial disease did not cause any significant alterations in gene-expression levels in IgG-treated control mice (Fig. 3A). In contrast, the presence of extracranial disease resulted in altered expression of 4,154 genes in anti–PD-1/anti–CTLA-4–treated mice. This suggested that extracranial disease has significant impact on the intracranial tumor only in the
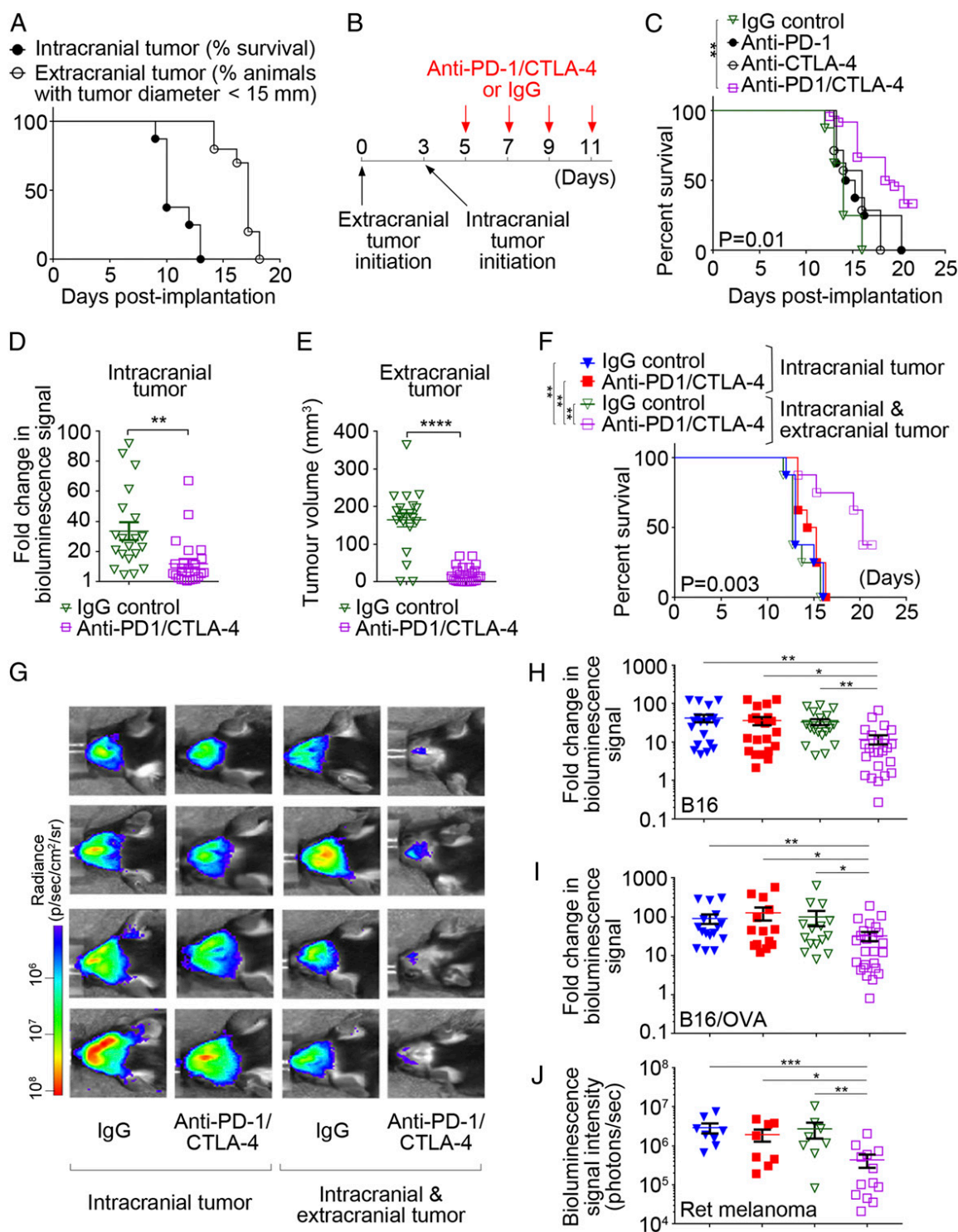
Fig. 1. Inhibition of intracranial tumor growth and prolonged survival following anti–PD-1/CTLA-4 therapy require the presence of extracranial disease. (*A*) Survival of C57BL/6J mice following intracranial implantation of B16/Fluc melanoma cells (*n* = 8) and time to the establishment of extracranial B16 subcutaneous tumors with a diameter of 15 mm (*n* = 10). (*B*) Experimental time line for the implantation of cancer cells in B16 model and therapeutic schedule. (*C*) Survival of mice with intracranial (B16/Fluc) plus extracranial (B16) tumors following the administration of anti–PD-1, anti–CTLA-4, anti–PD-1/CTLA-4, or IgG control (*n* = 8). The overall significance is shown. Individual *P* values are given in Fig. S1*C*. (*D*) Quantification of intracranial B16/Fluc tumor burden via bioluminescence imaging (*n* = 20/24). Fold-change in bioluminescence signal intensity between days 12 and 5 (e.g., pre/posttreatment) for mice treated with anti–PD-1/CTLA-4 or IgG. (*E*) Quantification of extracranial B16 tumor burden on day 12 via caliper measurement (*n* = 20/24). (*F*) Survival following anti–PD-1/anti–CTLA-4 or IgG administration was compared between mice bearing only intracranial B16/Fluc tumors and mice bearing intracranial B16/Fluc and extracranial B16 tumors. The overall significance is indicated. Individual *P* values are summarized in Fig. S1*D*. (*G*) Representative images of intracranial bioluminescence signals (B16/Fluc tumors). (*H* and *I*) Fold-change in intracranial bioluminescence signal intensity between days 12 and 5 (e.g., pre/posttreatment) for the B16/Fluc (*H*) and B16/OVA/Fluc (*I*) melanoma models (*n* = 21/21/20/24 for B16/Fluc; *n* = 16/16/15/25 for B16/OVA/Fluc). Labeling as in *F*. (*J*) Quantification of intracranial Ret/Fluc melanoma burden (*n* = 8/8/8/13). Bioluminescence signal intensity (total flux; photons per second) is shown. Labeling as in *F*. Significant differences in *C* and *F* were determined with log-rank test. Significant differences in *D*, *E*, and *H*–*J* were determined with a Mann–Whitney test (**P* ≤ 0.05; ***P* ≤ 0.01; ****P* ≤ 0.001; *****P* ≤ 0.0001). Data from two (*I*) or three (*C*–*F* and *H*) independent experiments are shown.
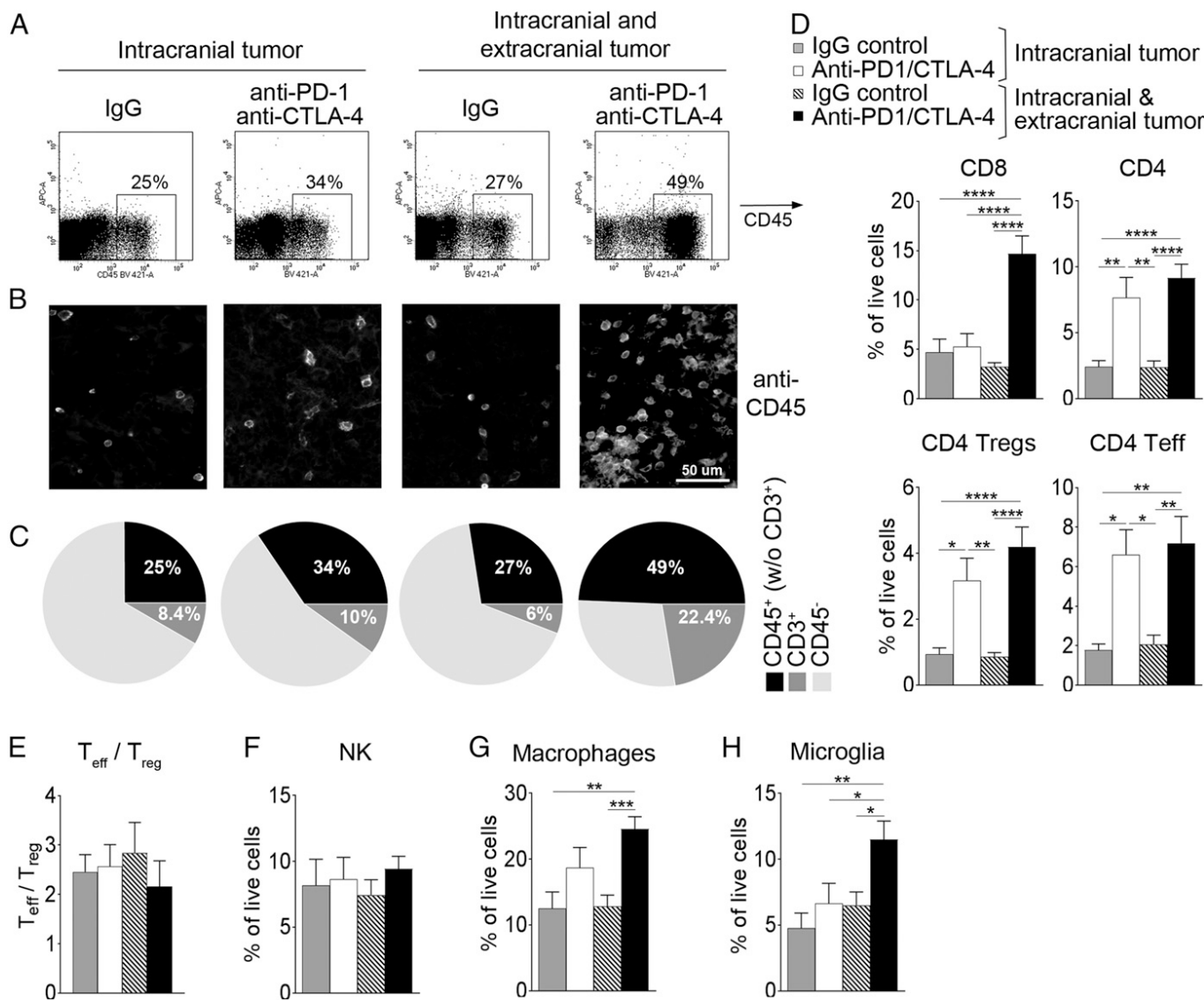
Fig. 2. Analysis of immune cell populations in intracranial B16 tumors reveals extracranial tumor- and PD-1/CTLA-4 blockade-dependent changes. (*A*) Representative dot plots of CD45$^+$ cell population. (*B*) Representative immunofluorescence images of CD45$^+$ cells infiltrating intracranial tumors. (*C*) Percentages of CD45$^+$ hematopoietic cells and CD3$^+$ T cells as quantified by flow cytometry. Significant *P* values are summarized in Fig. S2*B*. (*D–H*) Analysis of different T cell subpopulations (*D*), CD4$^+$ T$_{eff}$/T$_{reg}$ ratio (*E*), NK cells (*F*), CD11b$^+$F4/80$^+$CD45^{high} macrophages (*G*) and CD11b$^+$F4/80$^+$CD45^{low} microglia (*H*) within intracranial tumors by flow cytometry. Labeling as in *D*. All analyses were performed on day 12. Combined data from three independent experiments are shown (*n* = 10/13/16/24 per group for CD45$^+$, NK, microglia, and macrophages; *n* = 14/16/17/22 per group for T cell subpopulations). Significant differences were determined by ANOVA with a post hoc test (*$P \leq 0.05$; **$P \leq 0.01$; ***$P \leq 0.001$; ****$P \leq 0.0001$). Detailed ANOVA parameters are provided in Table S1.

context of PD-1/CTLA-4 blockade. By contrast, anti–PD-1/anti–CTLA-4 therapy itself had impact on gene expression both in the absence (906 differentially expressed genes) and presence (621 differentially expressed genes) of extracranial disease. Importantly, brain tumors from mice with intracranial and extracranial tumors undergoing anti–PD-1/anti–CTLA-4 treatment had significantly distinct transcriptomes compared with the other three experimental groups (Fig. 3*B*). Gene ontology (GO) enrichment analysis identified classes of genes significantly altered upon anti–PD-1/anti–CTLA-4 therapy in the presence of extracranial disease, revealing significant up-regulation in GO terms relating to NK cell activation and chemotaxis (Fig. 3*C*), T cell activation (Fig. 3*D* and Fig. S4*A*), and microglia/macrophage activation and migration (Fig. 2*E* and Fig. S4*B*).

Hence, our data revealed that anti–PD-1/anti–CTLA-4 efficacy in the brain correlates with intratumoral increase in CD8$^+$

T cells, macrophages, and microglia, as well as up-regulation of genes involved in activation of T cells, NK cells, and microglia/macrophages. This implies that anti–PD-1/anti–CTLA-4 activity relies on multiple immune cell populations, the activation or intratumoral increase of which were dependent on the presence of extracranial tumor.

CD8$^+$ T Cells and NK Cells Are Required for the Intracranial Efficacy of Anti–PD-1/Anti–CTLA-4 Therapy. The up-regulation of T cell and NK cell activation markers in association with the intracranial anti–PD-1/anti–CTLA-4 efficacy prompted us to investigate the functional role of these cell populations in the context of PD-1/CTLA-4 blockade. Antibody-mediated depletion of NK cells, CD4$^+$ or CD8$^+$ T cells was performed in mice bearing intracranial and extracranial B16 tumors undergoing anti–PD-1/anti–CTLA-4 therapy (Fig. 4*A*). Efficient depletion of respective
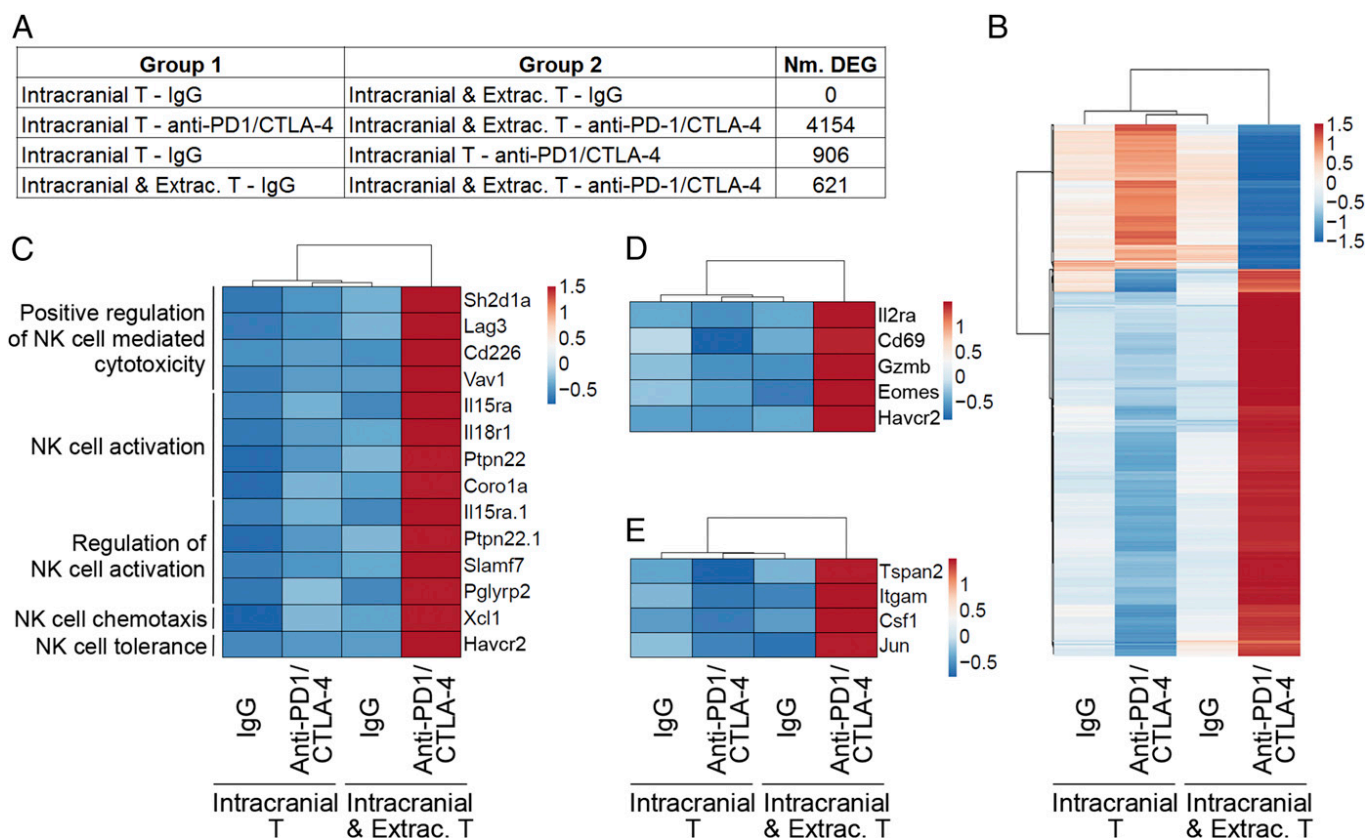
Fig. 3. PD-1/CTLA-4 blockade- and extracranial disease-dependent molecular changes within intracranial B16 tumors. (*A*) Number of genes differentially expressed within intracranial tumors between experimental groups. (*B*) Unsupervised hierarchical clustering and heat map of top 2,000 differentially expressed genes. (*C–E*) Unsupervised hierarchical clustering and heat maps of differentially expressed genes involved in NK cell function (*C*; the list of genes is based on the significantly enriched GO terms displayed on the *Left*), T cell function (*D*; example genes are shown; heat map including all genes is given in Fig. S4*B*), and microglia (*E*). The analysis was performed on day 12.

cell populations in the blood and tumor tissue was confirmed by flow cytometry (Fig. S5). While the depletion of CD4$^+$ T cells had no impact on survival (Fig. 4*B*), depletion of either NK (Fig. 4*D*) or CD8$^+$ T cells (Fig. 4*C*) resulted in a significant loss of survival advantage observed upon anti–PD-1/anti–CTLA-4 therapy, demonstrating a critical involvement of these cell populations.

To further characterize T cells in intracranial B16 tumors, we analyzed the expression of known T cell activation/exhaustion markers [e.g., CD25, CD69, Granzyme B, Eomesodermin (EOMES), T-cell Ig, and mucin domain containing-3 (TIM3)] in CD4$^+$ and CD8$^+$ T cells by flow cytometry (Fig. S6*A*). We detected no changes in the percentages of cells expressing the investigated markers or in their protein expression levels (mean fluorescence intensity, MFI) (Fig. S6 *B and C*). Therefore, marked increase in the overall gene-expression levels of T cell activation markers following anti–PD-1/anti–CTLA-4 therapy in the presence of extracranial tumor (Fig. 3*D*) can be explained by the increased intratumoral percentage of CD8$^+$ T cells (Fig. 2*D*). Our findings thus imply that inhibition of intracranial tumor growth was caused by an increase in CD8$^+$ T cell numbers rather than their enhanced intratumoral activation.

Anti–PD-1/Anti–CTLA-4 Treatment Enhances Trafficking of CD8$^+$ T Cells to Intracranial Tumors. We next sought to determine the underlying mechanism for the increase in intratumoral CD8$^+$ T cells following anti–PD-1/anti–CTLA-4 therapy. The proportion of proliferative CD8$^+$ T cells within intracranial B16 tumors was high (~75% Ki67$^+$ cells) and remained unaffected by anti–PD-1/anti–CTLA-4 treatment or the presence of extracranial disease (Fig. 5*A*). This finding excluded intra-

tumoral expansion of CD8$^+$ T cells as a major driver of their intratumoral increase. We therefore reasoned that enhanced recruitment of CD8$^+$ T cells from outside the brain is likely responsible for their accumulation in intracranial tumors following PD-1/CTLA-4 blockade. To investigate this, we analyzed the trafficking of CD8$^+$ T cells to intracranial tumors by performing an adoptive transfer of Cell-Trace Violet (CTV)-labeled CD8$^+$ T cells (4×10^6) in mice with extracranial plus intracranial tumors. T cell donor and recipient mice both received two doses of anti–PD-1/anti–CTLA-4 or IgG (Fig. 5*B*), which was sufficient to significantly increase the overall percentage of intratumoral CD8$^+$ T cells in treated compared with control mice (Fig. S8*A*). CD8$^+$ T cells from IgG-treated donor mice were transferred into IgG-treated recipient mice, and cells from anti–PD-1/anti–CTLA-4–treated donor mice were transferred into anti–PD-1/anti–CTLA-4–treated recipient mice (Fig. 5*B*). Analysis of intratumoral CTV$^+$ CD8$^+$ T cells at 18 h postadoptive transfer demonstrated a strong increase (~14-fold) in CD8$^+$ T cell homing to intracranial tumors in the presence of anti–PD-1/anti–CTLA-4 therapy (Fig. 5 *C and D*). Notably, we observed no significant proliferation of adoptively transferred T cells within 18 h, and therefore increase in intratumoral CTV$^+$ CD8$^+$ T cells was attributable exclusively to their trafficking and not their proliferation (Fig. S8*B*).

To investigate whether systemic T cell expansion may contribute to enhanced accumulation of CD8$^+$ T cells in intracranial B16 tumors, we analyzed peripheral T cell populations in the blood and spleens. All anti–PD-1/anti–CTLA-4–dependent changes in ratios of peripheral CD8$^+$ T cells, CD4$^+$ T$_{eff}$, and T$_{reg}$ cells occurred independently of extracranial disease (Fig. S7). In contrast, PD-1/CTLA-4 blockade-induced increase in CD44$^+$CD62L$^-$ effector CD8$^+$ T cells in blood was significantly enhanced in the presence
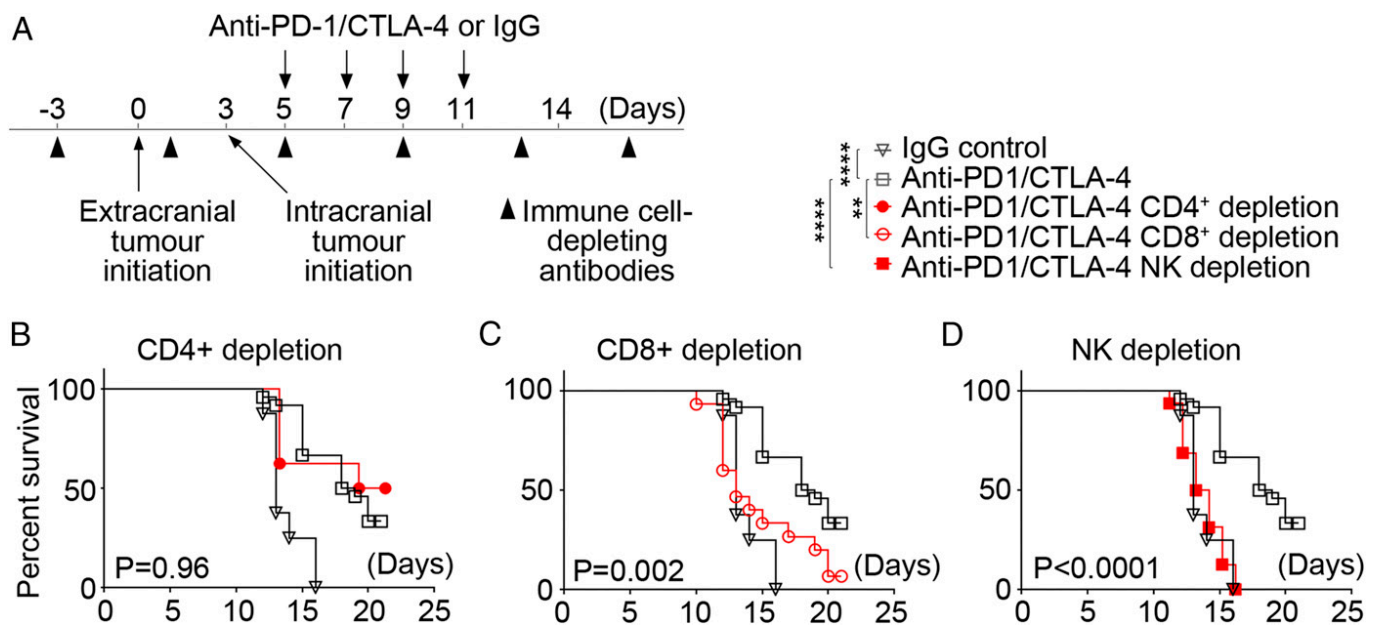
Fig. 4. CD8^{+} T cells and NK cells are required for intracranial efficacy of PD-1/CTLA-4 blockade in B16 model. (*A*) Experimental timeline indicating administration of respective immune cell-depleting antibodies. (*B–D*) Survival analysis of anti–PD-1/anti–CTLA-4-treated mice bearing intracranial and extracranial tumors following in vivo depletion of CD4^{+} T cells, CD8^{+} T cells, or NK cells, respectively (*n* = 16; pooled data from two independent experiments). Significant differences were determined with log-rank test. *P* values shown are for comparison between the anti–PD-1/CTLA-4 group and the respective group in which a specific immune cell population has been depleted; **$P \leq 0.01$; ****$P \leq 0.0001$.

of extracranial disease, and thus correlated with the intracranial anti–PD-1/anti–CTLA-4 efficacy (Fig. 5*E*). Analysis of intracranial tumors revealed that the majority of intratumoral CD8^{+} T cells were CD44^{+}CD62L^{−} effector cells in both treated and control mice (Fig. 5*F*). This prompted us to compare homing of CD44^{+}CD62L^{−} effector and CD44^{−}CD62L^{+}-naïve CD8^{+} T cells to intracranial tumors. Notably, the percentage of CD8^{+} T cells within pooled spleen and lymph nodes was slightly higher in anti–PD-1/anti–CTLA-4–treated mice (10.3%) compared with the IgG-treated mice (9%) (Fig. 5*G*, *Upper*). Moreover, the percentage of CD44^{+}CD62L^{−} cells within CD8^{+} T cell population was higher in anti–PD-1/anti–CTLA-4–treated mice (3.8%) compared with IgG-treated mice (2.2%) (Fig. 5*G*, *Lower*). Thus, to ensure that the same numbers of cells per investigated CD8^{+} T cell population are used for adoptive transfer in the control and therapy group, we sorted CD44^{+}CD62L^{−} and CD44^{−}CD62L^{+} CD8^{+} T cell populations from pooled spleens and lymph nodes of IgG- and anti–PD-1/anti–CTLA-4–treated mice, respectively. CTV-labeled CD44^{+}CD62L^{−} (1×10^5) and CD44^{−}CD62L^{+} (2.4×10^6) cells, respectively, were transferred into recipient mice that received the corresponding treatment (Fig. 5*B*). Analysis of CTV^{+} CD8^{+} T cells within intracranial tumors at 18 h posttransfer confirmed that only CD44^{+}CD62L^{−} cells efficiently homed to intracranial tumors (Fig. 5*H*). Notably, we detected a tendency toward more efficient homing of CD44^{+}CD62L^{−} CD8^{+} T cells isolated from anti–PD-1/anti–CTLA-4–treated mice (0.009 ± 0.004% all cells) compared with the IgG control mice (0.006 ± 0.002% all cells) (Fig. 5*I*). In summary, this suggested that an enhanced homing of CD8^{+} T cells to intracranial tumors following anti–PD-1/anti–CTLA-4 therapy is mainly due to the peripheral expansion of CD44^{+}CD62L^{−} effector cells. However, a tendency toward more efficient homing of effector CD8^{+} T cells isolated from anti–PD-1/anti–CTLA-4–treated mice compared with IgG-treated mice implied that additional factors may be involved.

PD-1/CTLA-4 Blockade Up-Regulates T Cell Trafficking Determinants on Tumor Blood Vessels. Consistent with a tendency toward increased trafficking of CD8^{+} effector T cells to intracranial tumors

following anti–PD-1/anti–CTLA-4 treatment, Kyoto Encyclopedia of Genes and Genomes (KEGG) pathway analysis identified "Leukocyte transendothelial migration" as one of the pathways significantly up-regulated in intracranial tumors following PD-1/CTLA-4 blockade in the presence of extracranial disease compared with the other three experimental groups (Fig. 6*A*). Among the up-regulated genes, vascular cell adhesion molecule 1 (*Vcam1*) and intercellular adhesion molecule 1 (*Icam1*)—two major endothelial T cell entry receptors (33)—were up-regulated 6.4- and 3.8-fold, respectively (Fig. 6*A*). VCAM-1 expression on tumor blood vessels was confirmed by immunofluorescence (Fig. 6*B*). Analysis of VCAM-1 and ICAM-1 expression on tumor endothelial cells by flow cytometry confirmed a significant up-regulation of both receptors following anti–PD-1/anti–CTLA-4 therapy in the presence of extracranial disease (Fig. 6 *C* and *D* and Fig. S8*C*). The percentage of ICAM-1^{+} endothelial cells increased from ~75 to 90% and the percentage of VCAM-1^{+} endothelial cells from ~5 to 45%. Moreover, the expression levels of both receptors were ~threefold elevated, as indicated by a significant increase in MFI (Fig. 6*D*).

Following anti–PD-1/anti–CTLA-4 therapy, blood vessels within the tumor-adjacent brain parenchyma remained negative for VCAM-1 expression (Fig. S8*D*), indicating that the up-regulation of T cell entry receptors was restricted to the tumor microenvironment. In line with this finding, gene-expression levels of *Ifnγ*, a known inducer of endothelial VCAM-1 and ICAM-1 (33), were up-regulated within intracranial tumors following anti–PD-1/anti–CTLA-4 therapy in mice bearing tumors at both sites (Fig. S8*E*). Concurrently, intracellular flow cytometry staining revealed a significant increase in the percentage of IFN-γ^{+} cells within NK cell and macrophage populations (Fig. 6*E*, *Upper*), while TNF-α expression remained unaltered (Fig. S8*F*). Although such an increase in IFN-γ expression was not detected for CD8^{+} T cells and microglia, their increased proportion within intracranial tumors per se also contributed toward an overall increase in IFN-γ (Fig. 6*E*, *Lower*).

In summary, our data indicate that anti–PD-1/anti–CTLA-4 treatment—in the context of clinically relevant extracranial disease—increases intratumoral CD8^{+} T cells in the brain through
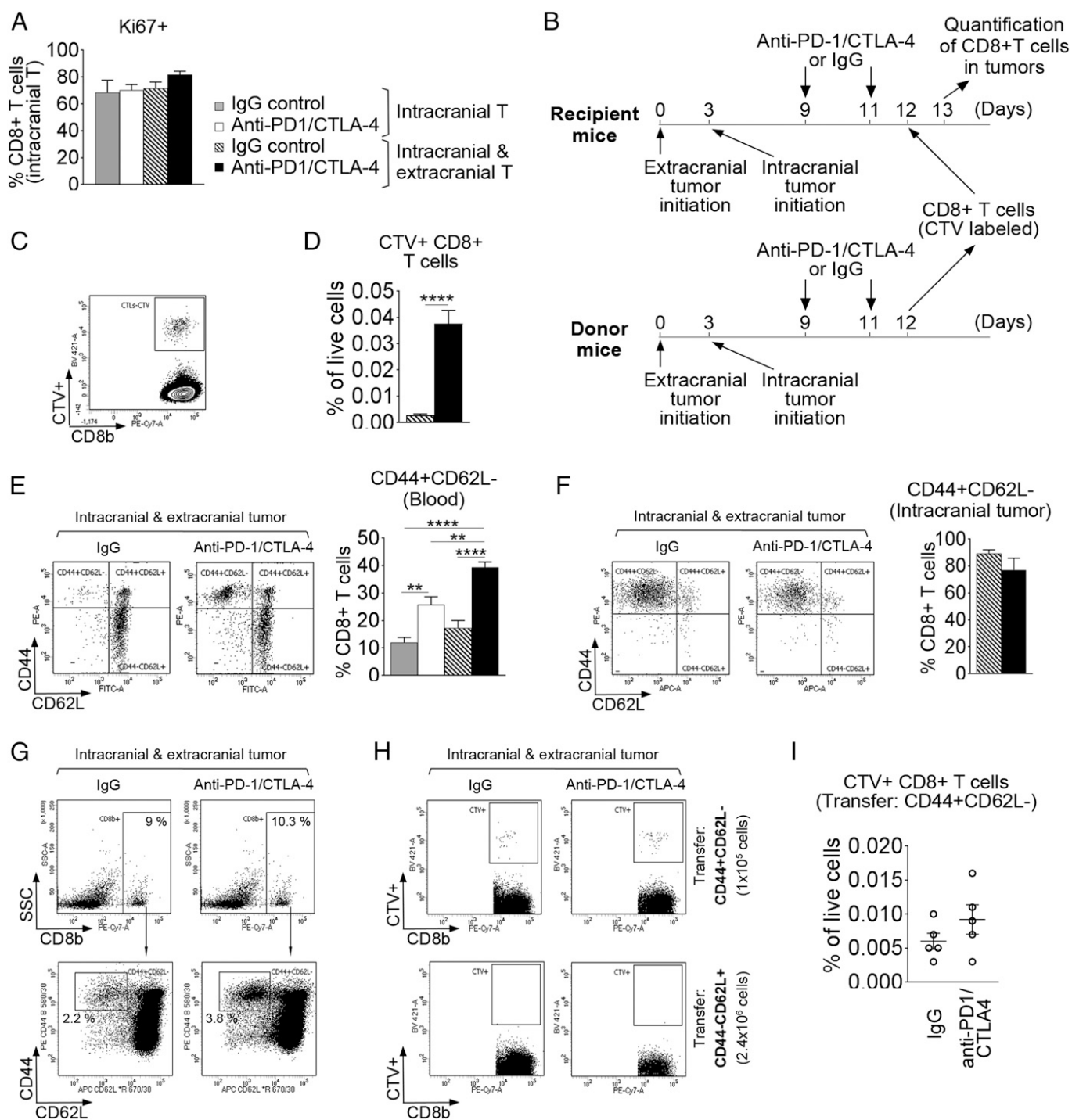
Fig. 5. Anti–PD-1/anti–CTLA-4 therapy in the context of extracranial disease potentiates trafficking of CD8⁺ T cells to intracranial B16 tumors. (A) Analysis of Ki67⁺ CD8⁺ T cells within intracranial tumors by flow cytometry. (B) Schematic representation of adoptive transfer experiments using CTV-labeled CD8⁺ T cells. (C) Representative dot plot of adoptively transferred CTV⁺ CD8⁺ T cells detected within intracranial tumors. (D) Analysis of adoptively transferred CTV⁺ CD8⁺ T cells in intracranial tumors at 18 h posttransfer (n = 10). Labeling as in A. (E and F) Analysis of CD44⁺CD62L⁻ CD8⁺ effector T cells in blood (E) and intracranial tumors (F) on day 12 (n = 6/6/7/12 for blood; n = 10/10 for intracranial tumors). Labeling as in A. (G) Dot plots of pooled spleen and lymph node cells isolated from donor mice for use in adoptive CD8⁺ T cell transfer experiments. Percentages of total CD8⁺ T cells and CD44⁺CD62L⁻ cells within the CD8⁺ T cell population are indicated. (H) Representative dot plots of adoptively transferred CTV-tagged CD44⁺CD62L⁻ (Upper) and CD44⁻CD62L⁺ (Lower) CD8⁺ T cells detected within intracranial tumors at 18 h posttransfer. (I) Analysis of adoptively transferred CTV-tagged CD44⁺CD62L⁻ CD8⁺ T cells in intracranial tumors at 18 h posttransfer (n = 5). Significant differences in A and E were determined by ANOVA with a post hoc test, and in D, F, and I with a two-tailed t-test (unequal variance); **P ≤ 0.01; ****P ≤ 0.0001. Data from at least two repeat experiments were pooled for analysis (A–F). Detailed ANOVA and t-test parameters are provided in Tables S1 and S2.

peripheral expansion of CD44⁺CD62L⁻ effector CD8⁺ T cells and potentiation of their trafficking to intracranial tumors, the latter potentially occurring via up-regulation of T cell entry receptors ICAM-1/VCAM-1 on the tumor vasculature.

Discussion

In this study, we reveal that extracranial disease plays a critical role for the intracranial efficacy of combined anti–PD-1 plus anti–CTLA-4 therapy. This was demonstrated through analysis
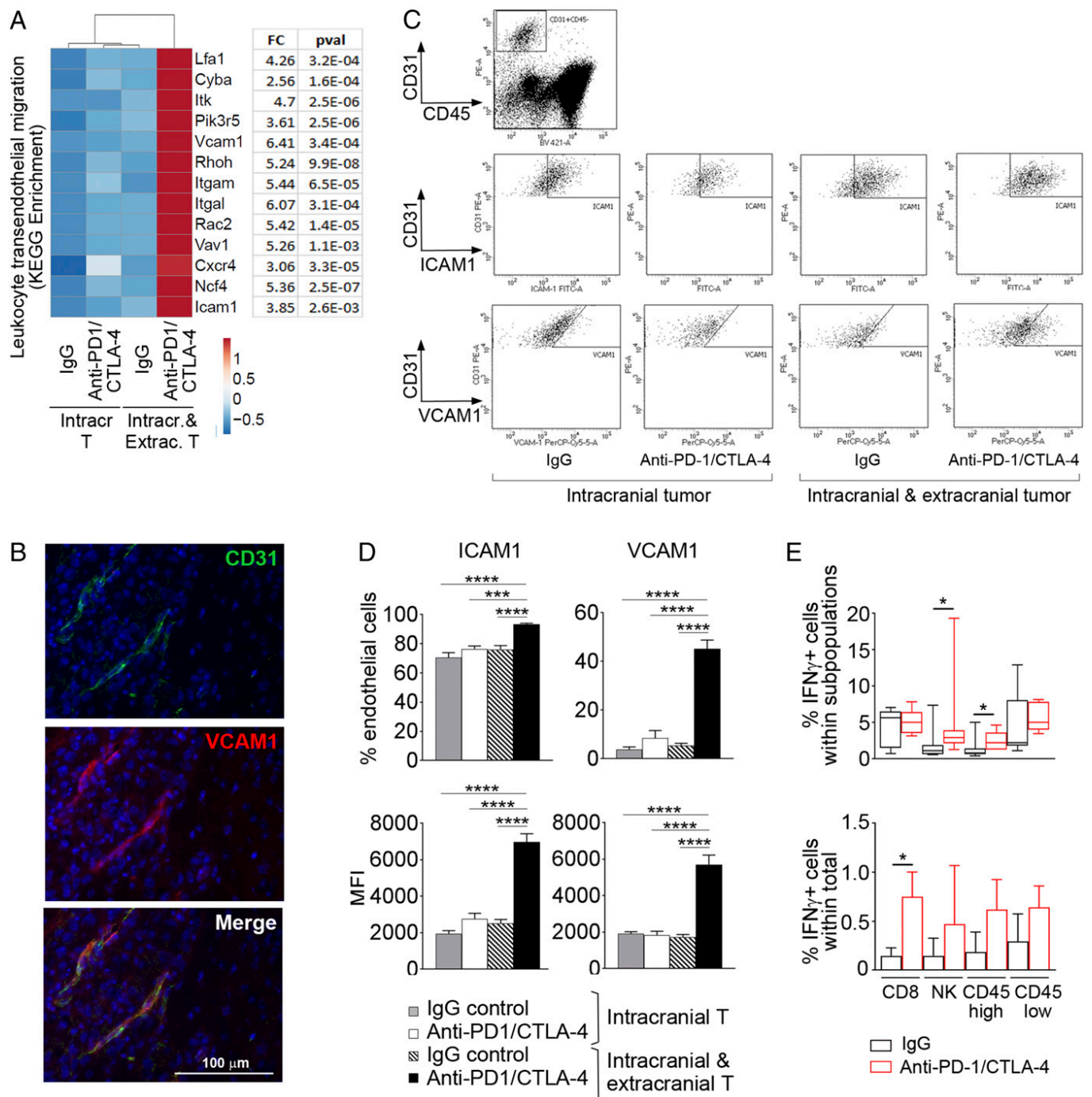
Fig. 6. PD-1/CTLA-4 blockade up-regulates vascular T cell trafficking determinants in intracranial B16 tumors. (*A*) Unsupervised hierarchical clustering and heat map of genes differentially expressed within the "Leukocyte transendothelial migration" KEGG pathway. FC, fold-change; pval, *P* value. (*B*) Immunofluorescence staining for CD31 (endothelial cells) and VCAM-1 within intracranial tumors from treated mice bearing intracranial and extracranial tumors. (*C*) Representative dot plots of endothelial cells (CD45⁻CD31⁺) and ICAM-1/VCAM-1 staining within the endothelial cell population. (*D*) Analysis of ICAM-1 and VCAM-1 expression in intracranial tumors by flow cytometry (*n* = 5/5/7/9). One of two representative experiments is shown. (*E*) Analysis of intracellular IFN-γ staining in intracranial tumors isolated from Brefeldin A-treated mice (*n* = 7). Percentage of IFN-γ⁺ cells within respective immune cell populations (*Upper*) and within total cell population (*Lower*) is shown. Data from two independent experiments were pooled for analysis. Significant differences in *D* and *E*, *Lower* were determined by ANOVA with a post hoc test, and in *E*, *Upper* with Mann–Whitney *U* Test (one-tailed, *P ≤ 0.05); ***P ≤ 0.001; ****P ≤ 0.0001. Detailed ANOVA parameters are provided in Table S1.

of intracranial tumor-dependent survival, quantification of tumor growth, characterization of tumor-infiltrating immune cell populations, and gene-expression analysis (mRNAseq). Importantly, clinically observed intracranial activity of anti–PD-1/anti–CTLA-4 therapy (4, 5, 11–15) could be recapitulated only in the tumor transplantation model with intracranial plus extracranial

tumor, but not in the model bearing only intracranial cancer lesions, which is a conventional brain tumor transplantation model (17, 27). Moreover, superior intracranial activity of anti–PD-1/anti–CTLA-4 combination therapy in our optimized model was in line with the reported higher intracranial response rates with combined anti–PD-1 plus anti–CTLA-4 (50%) than anti–PD-1 alone

(21%) in drug-treatment naïve patients (15). Thus, by including extracranial tumor, we achieved an important improvement in simulating human disease and clinical responses to PD-1 and CTLA-4 blockade in the brain, and thus our model is expected to significantly advance preclinical studies on immunotherapy in BrM.

In terms of adaptive immune responses, the brain is markedly different from other major sites of metastasis, such as the skin, lungs, and bones (26). While antigens from these other sites are efficiently transported to the peripheral lymphoid organs where T cell priming/activation occurs, a body of literature shows that antigens located within the brain are less accessible and transported to lymph nodes at a different location (e.g., cervical lymph nodes) or presented in a different way (20–23). In line with this notion, our study reveals that successful targeting of melanoma BrM with anti–PD-1/anti–CTLA-4 antibodies relies on: (i) tumor antigens present at extracranial locations and (ii) release of CD8$^+$ T cells from ICI and their activation occurring outside the brain. Notably, release of T cells from ICI and their subsequent increased proliferation following anti–CTLA-4 and anti–PD-1 therapy is mainly observed within secondary lymphoid organs and within the tumor microenvironment, respectively (14). Accordingly, increase in proliferation of intratumoral CD8$^+$ T cells occurs in subcutaneous B16 melanoma tumors following PD-1 blockade alone or in combination with anti–CTLA-4 or radiotherapy (34–36). However, in contrast to extracranial sites, the blood–brain barrier limits access of therapeutic antibodies into brain tumors, which may preclude anti–PD-1–induced release of T cells from proliferation block once they have entered the brain tumor microenvironment. Indeed, in our study, anti–PD-1/anti–CTLA-4 combination failed to increase the proportion of proliferative CD8$^+$ T cells and their expression of activation markers within intracranial tumors. This provides strong evidence that the release of CD8$^+$ T cells from ICI occurred mainly outside the brain, and that intracranial anti–PD-1/anti–CTLA-4 activity relies on the subsequent recruitment of these extracranially activated CD8$^+$ T cells to intracranial tumors.

Our data suggest that enhanced CD8$^+$ T cell trafficking to intracranial tumors following anti–PD-1/anti–CTLA-4 therapy in the context of extracranial disease may be enhanced through the up-regulation of VCAM-1 and ICAM-1 on tumor blood vessels. IFN-γ was identified as one of the potential factors involved in the up-regulation of these vascular receptors. NK cells and microglia/macrophages were the main source of anti–PD-1/anti–CTLA-4–induced IFN-γ up-regulation. This finding may explain why intracranial anti–PD-1/anti–CTLA-4 efficacy required NK cells and correlated with intratumoral increase in macrophages. Notably, the latter may have been recruited to intracranial tumors through colony stimulating factor 1 (CSF-1), a potent microglia/macrophages chemoattractant (37), which—in our study—was found to be up-regulated 2.8-fold following anti–PD-1/anti–CTLA-4 therapy in the presence of extracranial tumor. Several studies reported IFN-γ increase in tumors following ICI treatment, although this has not yet been connected to the up-regulation of vascular T cell homing determinants or enhanced T cell trafficking (34, 36, 38). Nevertheless, IFN-γ–dependent up-regulation of ICAM-1 on choroid plexus epithelial cells in the brain has been recently shown to increase T cell infiltration into the brain in models of spinal cord injury and Alzheimer's disease (39, 40).

More than half of patients with metastatic melanoma develop BrM and, with ICI becoming the frontline therapy for metastatic disease, it is critical to understand how ICI can be optimized in the brain. Because the intracranial anti–PD-1/anti–CTLA-4 efficacy seemed to rely on the recruitment of activated CD8$^+$ T cells from outside the brain, strategies aimed at enhancing T cell homing—for example, through adoptive T cell therapy using T cells with enhanced BrM-homing characteristics—have a strong potential to improve the efficacy of ICI in the brain. Moreover, our findings on the critical role of extracranial disease for intracranial anti–PD-1/anti–CTLA-4 efficacy are of relevance to the optimization of ICI for primary nonmetastatic brain cancers, in particular glioma. Notably, in contrast to clinical evidence for anti–PD-1 activity in melanoma BrM (12, 13), a recent phase III clinical trial of nivolumab in glioma was negative (https://news.bms.com/press-release/bmy/bristol-myers-squibb-announces-results-checkmate-143-phase-3-study-opdivo-nivoluma). Our data suggest that the combination of ICI with strategies that boost the peripheral antigen-specific T cell activation, such as cancer vaccines, may also improve anti–PD-1/anti–CTLA-4 efficacy in metastatic and nonmetastatic brain cancers.

Materials and Methods

In Vivo Model of Brain Metastases. All procedures were approved by the University of Leeds Animal Welfare and Ethical Review Committee and performed under the approved United Kingdom Home Office project license in line with the Animal (Scientific Procedures) Act 1986 and in accordance with the United Kingdom National Cancer Research Institute Guidelines for the welfare of animals (41).

Six- to 8-wk-old female C57BL/6J or B6N-Tyrc-Brd/BrdCrCrl (B6 Albino) mice were purchased from Charles River Laboratories, UK. B16 F1, B16/OVA, or Ret melanoma cells (please refer to *SI Materials and Methods* for cell line details) were injected subcutaneously on the flank to generate extracranial tumors (2 × 10^5 B16 and B16/OVA cells; 1 × 10^5 Ret cells). To generate intracranial tumors, cancer cells (1 × 10^5 B16/Fluc and B16/OVA/Fluc cells; 1 × 10^3 Ret/Fluc cells) were stereotactically injected into the striatum (2-mm right from the midline, 2-mm anterior from bregma, 3-mm deep). Before treatment, mice used in experiments with B16 and B16/OVA models were randomized into groups based on the intracranial bioluminescence signals ensuring equal distribution of tumor burden across groups. Mice used in experiments with the Ret melanoma model were randomized into groups so as to ensure an equal proportion of mice from different litters per group (randomization based on the bioluminescence signal intensity was not possible at early time points due to the low number of implanted cells in this model). Anti–PD-1 (RMP1-14), anti–CTLA-4 (9D9), and IgG control (MPC11) were purchased from Bio-X-Cell and administered intraperitoneally at 200 μg per mouse, as indicated.

Experimental group sizes were determined with power analysis (power = 80%, significance level = 5%, difference to be detected between groups = 50%) using the mean values and SDs from our pilot studies. All animals were included in the survival analysis and tumor growth analysis. In cases where tumors were too small to obtain sufficient material for FACS analysis, the animals were excluded from this analysis. All outliers were included in the analysis. The study was not blinded.

Quantification of extracranial tumor growth was performed by caliper measurement. Quantification of intracranial tumor growth was performed via noninvasive bioluminescence imaging using IVIS Spectrum and Living Image software (PerkinElmer).

Immune cell depletion was achieved through intraperitoneal administration of anti-CD8α (YTS.4; Bio-X-Cell), anti-CD4 (GK1.5; Bio-X-Cell), or antiasialo-GM1 that depletes NK cells (polyclonal rabbit IgG; Cedarlane) at 100 μg per mouse every 4 d. For detection of IFN-γ and TNF-α by flow cytometry, mice received 250 μg Brefeldin A (Sigma) intravenously 6 h before tissue harvesting. Adoptive T cell transfer experiments are described in *SI Materials and Methods*.

Immunofluorescence. Immunofluorescence was performed as previously described (25). Details are provided in *SI Materials and Methods*.

Flow Cytometry. Mice were perfused with saline. Tumors were mechanically disrupted and enzymatically dissociated (25). The blood (collected from tail vein) and splenocytes were treated with ammonium-chloride-potassium buffer to lyse red blood cells. Samples were blocked with 10% rat serum and FcR blocking reagent (Miltenyi) before surface antigen staining. FoxP3/Transcription Factor Staining Buffer Set (eBioscience) was used for intracellular staining of nuclear antigens following the manufacturer's instructions. Intracellular fixation buffer and Permeabilization buffer (eBioscience) were used for staining of cytoplasmic antigens following manufacturer's instructions. Cells were analyzed on BD LSRII Flow Cytometry Analyzer (Life Technologies). Data were quantified using FACSDiva software. The gates were set based on appropriate isotype controls. Antibody details are provided in *SI Materials and Methods*.

RNAseq and Gene-Expression Analysis. Details of RNAseq and gene-expression analysis are provided under *SI Materials and Methods*.

Statistical Analysis. Statistical analysis was carried out using Graph Pad Prism v7 (Graph Pad Software). Statistical tests used were ANOVA with a post hoc test for multiple comparisons (Tukey's multiple comparisons test), Mann–Whitney test, and Mann–Whitney *U* test, as specified in figure legends. All tests except the Mann–Whitney *U* test were two-tailed statistical tests. Statistical significance in survival experiments was determined with log-rank test. Error bars represent SEM, except in Fig. 6*E*, *Upper*, where the bars represent SDs. The number of biological replicates for each experiment is stated in figure legends. Each experiment was performed two to four times, as specified. Data from repeat experiments were combined as indicated in the figure legends.

1. Davies MA, et al. (2011) Prognostic factors for survival in melanoma patients with brain metastases. *Cancer* 117:1687–1696.
2. Long GV, Margolin KA (2013) Multidisciplinary approach to brain metastasis from melanoma: The emerging role of systemic therapies. *Am Soc Clin Oncol Educ Book* 2013:393–398.
3. Sampson JH, Carter JH, Jr, Friedman AH, Seigler HF (1998) Demographics, prognosis, and therapy in 702 patients with brain metastases from malignant melanoma. *J Neurosurg* 88:11–20.
4. Ajithkumar T, Parkinson C, Fife K, Corrie P, Jefferies S (2015) Evolving treatment options for melanoma brain metastases. *Lancet Oncol* 16:e486–e497.
5. Puzanov I, Wolchok JD, Ascierto PA, Hamid O, Margolin K (2013) Anti-CTLA-4 and BRAF Inhibition in patients with metastatic melanoma and brain metastases. *Expert Rev Dermatol* 8:479–487.
6. Kamphorst AO, Ahmed R (2013) Manipulating the PD-1 pathway to improve immunity. *Curr Opin Immunol* 25:381–388.
7. Walker LS, Sansom DM (2011) The emerging role of CTLA4 as a cell-extrinsic regulator of T cell responses. *Nat Rev Immunol* 11:852–863.
8. Larkin J, et al. (2015) Combined nivolumab and ipilimumab or monotherapy in untreated melanoma. *N Engl J Med* 373:23–34.
9. Boutros C, et al. (2016) Safety profiles of anti-CTLA-4 and anti-PD-1 antibodies alone and in combination. *Nat Rev Clin Oncol* 13:473–486.
10. Berghoff AS, Venur VA, Preusser M, Ahluwalia MS (2016) Immune checkpoint inhibitors in brain metastases: From biology to treatment. *Am Soc Clin Oncol Educ Book* 35:e116–e122.
11. Margolin K, et al. (2012) Ipilimumab in patients with melanoma and brain metastases: An open-label, phase 2 trial. *Lancet Oncol* 13:459–465.
12. Goldberg SB, et al. (2016) Pembrolizumab for patients with melanoma or non-small-cell lung cancer and untreated brain metastases: Early analysis of a non-randomised, open-label, phase 2 trial. *Lancet Oncol* 17:976–983.
13. González-Cao M, et al.; Spanish Melanoma Group (2017) Pembrolizumab for advanced melanoma: Experience from the Spanish Expanded Access Program. *Clin Transl Oncol* 19:761–768.
14. Parakh S, et al. (2017) Efficacy of anti-PD-1 therapy in patients with melanoma brain metastases. *Br J Cancer* 116:1558–1563.
15. Long GV, et al. (2017) A randomized phase II study of nivolumab or nivolumab combined with ipilimumab in patients (pts) with melanoma brain metastases (mets): The Anti-PD1 Brain Collaboration (ABC). *J Clin Oncol* 35(Suppl):9508 (abstr).
16. Tawbi H, et al. (2017) Efficacy and safety of nivolumab plus ipilimumab in patients with melanoma metastatic to the brain: Results of the phase II study CheckMate 204. *J Clin Oncol* 35(Suppl):9507 (abstr).
17. Cohen JV, et al. (2016) Melanoma central nervous system metastases: Current approaches, challenges, and opportunities. *Pigment Cell Melanoma Res* 29:627–642.
18. Cho JH, et al. (2015) AKT1 activation promotes development of melanoma metastases. *Cell Rep* 13:898–905.
19. Schwartz H, et al. (2016) Incipient melanoma brain metastases instigate astrogliosis and neuroinflammation. *Cancer Res* 76:4359–4371.
20. Binder DC, Davis AA, Wainwright DA (2015) Immunotherapy for cancer in the central nervous system: Current and future directions. *OncoImmunology* 5:e1082027.
21. Carson MJ, Doose JM, Melchior B, Schmid CD, Ploix CC (2006) CNS immune privilege: Hiding in plain sight. *Immunol Rev* 213:48–65.
22. Ransohoff RM, Engelhardt B (2012) The anatomical and cellular basis of immune surveillance in the central nervous system. *Nat Rev Immunol* 12:623–635.
23. Harling-Berg CJ, Park TJ, Knopf PM (1999) Role of the cervical lymphatics in the Th2-type hierarchy of CNS immune regulation. *J Neuroimmunol* 101:111–127.
24. Alonso-Camino V, et al. (2014) The profile of tumor antigens which can be targeted by immunotherapy depends upon the tumor's anatomical site. *Mol Ther* 22:1936–1948.
25. Rippaus N, et al. (2016) Metastatic site-specific polarization of macrophages in intracranial breast cancer metastases. *Oncotarget* 7:41473–41487.
26. Tas F (2012) Metastatic behavior in melanoma: Timing, pattern, survival, and influencing factors. *J Oncol* 2012:647684.
27. Damsky WE, Theodosakis N, Bosenberg M (2014) Melanoma metastasis: New concepts and evolving paradigms. *Oncogene* 33:2413–2422.
28. Merrick A, et al. (2008) Autologous versus allogeneic peptide-pulsed dendritic cells for anti-tumour vaccination: Expression of allogeneic MHC supports activation of antigen specific T cells, but impairs early naïve cytotoxic priming and anti-tumour therapy. *Cancer Immunol Immunother* 57:897–906.
29. Zhao F, et al. (2009) Activation of p38 mitogen-activated protein kinase drives dendritic cells to become tolerogenic in ret transgenic mice spontaneously developing melanoma. *Clin Cancer Res* 15:4382–4390.
30. Ford AL, Goodsall AL, Hickey WF, Sedgwick JD (1995) Normal adult ramified microglia separated from other central nervous system macrophages by flow cytometric sorting. Phenotypic differences defined and direct ex vivo antigen presentation to myelin basic protein-reactive CD4+ T cells compared. *J Immunol* 154:4309–4321.
31. Hickman SE, et al. (2013) The microglial sensome revealed by direct RNA sequencing. *Nat Neurosci* 16:1896–1905.
32. Simpson TR, et al. (2013) Fc-dependent depletion of tumor-infiltrating regulatory T cells co-defines the efficacy of anti-CTLA-4 therapy against melanoma. *J Exp Med* 210:1695–1710.
33. Prendergast CT, Anderton SM (2009) Immune cell entry to central nervous system—Current understanding and prospective therapeutic targets. *Endocr Metab Immune Disord Drug Targets* 9:315–327.
34. Peng W, et al. (2012) PD-1 blockade enhances T-cell migration to tumors by elevating IFN-γ inducible chemokines. *Cancer Res* 72:5209–5218.
35. Spranger S, et al. (2014) Mechanism of tumor rejection with doublets of CTLA-4, PD-1/PD-L1, or IDO blockade involves restored IL-2 production and proliferation of CD8(+) T cells directly within the tumor microenvironment. *J Immunother Cancer* 2:3.
36. Twyman-Saint Victor C, et al. (2015) Radiation and dual checkpoint blockade activate non-redundant immune mechanisms in cancer. *Nature* 520:373–377.
37. Coniglio SJ, et al. (2012) Microglial stimulation of glioblastoma invasion involves epidermal growth factor receptor (EGFR) and colony stimulating factor 1 receptor (CSF-1R) signaling. *Mol Oncol* 6:e519–527.
38. Das R, et al. (2015) Combination therapy with anti-CTLA-4 and anti-PD-1 leads to distinct immunologic changes in vivo. *J Immunol* 194:950–959.
39. Baruch K, et al. (2016) PD-1 immune checkpoint blockade reduces pathology and improves memory in mouse models of Alzheimer's disease. *Nat Med* 22:135–137.
40. Kunis G, et al. (2013) IFN-γ-dependent activation of the brain's choroid plexus for CNS immune surveillance and repair. *Brain* 136:3427–3440.
41. Workman P, et al.; Committee of the National Cancer Research Institute (2010) Guidelines for the welfare and use of animals in cancer research. *Br J Cancer* 102:1555–1577.
42. Trapnell C, et al. (2010) Transcript assembly and quantification by RNA-Seq reveals unannotated transcripts and isoform switching during cell differentiation. *Nat Biotechnol* 28:511–515.